The Astrophysical Journal, 678: L145–L148, 2008 May 10

EFFECTS OF SOLAR MAGNETIC ACTIVITY ON THE CHARGE STATES OF MINOR IONS OF SOLAR WIND

Xuyu Wang,[1] Berndt Klecker,[2] and Peter Wurz[3]

Received 2008 January 23; accepted 2008 March 31; published 2008 April 14

ABSTRACT

We present an investigation of the effects of solar magnetic activity on the charge states of minor ions (Fe, Si, Mg, Ne, O, C) in the solar wind using *ACE* solar wind data, the "current sheet source surface" (CSSS) model of the corona, and *SOHO* MDI data during the 23rd solar cycle. We find that the mean charge states indicate a clear trend of increasing with solar activity when the solar wind speed is above 550 km s^{-1}. At lower speeds, no significant solar activity dependence is found. When displayed as a function of solar wind speed, iron is different from other elements in that it displays lower charge states in slow wind than in fast wind. The percentages of the high charge states for species with higher m/q (Fe and Si) increase with the solar wind speed, while for the species with lower m/q (Mg, O, C), the percentages of the high charge states decrease with the solar wind speed.

Subject headings: solar wind — Sun: activity

Online material: color figures

1. INTRODUCTION

The magnetic field of the Sun includes two components: open magnetic flux, which opens into the heliosphere to form the heliospheric magnetic field; and closed magnetic flux, in the form of loops attached at both ends to the Sun. The open flux controls many of the important processes in the solar corona. Reames (1999) argues that the interaction of loops with open flux is essential for an impulsive solar particle event, triggering the redistribution of the magnetic field in the loop and the escape of energetic particles. The interaction and reconnection between open flux and coronal loops releases matter and energy from the closed onto open field lines, which may feed and power the solar wind. As a result, open flux is broadly distributed on the Sun (Fisk et al. 1999; Fisk 2003; Fisk & Zurbuchen 2006). The open flux also exhibits the reversal in polarity of the magnetic field over the Sun. The polarity of coronal mass ejection (CME) footpoints tends to follow a pattern similar to the Hale cycle of sunspot polarity; repeated CME eruption and subsequent reconnection will result in latitudinal transport of open flux and reverse the coronal fields (Owens et al. 2007). Understanding how the open flux of the Sun behaves, how it is transported and distributed, is important for understanding the coupling of the Sun and the heliosphere. The distribution of open flux can thus also be a sign of solar activity.

Solar wind charge states are indicative of the coronal electron temperature when assuming local thermodynamic equilibrium between the electrons and ions (Arnaud & Raymond 1992; Bryans et al. 2006). Each charge state pair freezes-in at a different altitude, where the coronal expansion timescale overcomes its ionization/recombination timescale. Recently studies of charge states in fast streams found that the inferred electron temperature given by the in situ observed charge states are higher than those derived from the spectroscopic measurements. To resolve this discrepancy, two assumptions were adopted: one is assuming a non-Maxwellian velocity distribution for electrons with a suprathermal tail in the near-Sun region (Aellig et al. 1999; Esser & Edgar 2000); the other is introducing a differential flow speed between the adjacent charge states of the same element with the assumption of a Maxwellian velocity distribution for the solar wind particles (Ko et al. 1997; Esser & Edgar 2001). However, Chen et al. (2003) found that the differential flow speed has no significant impact on the formation of most minor ions. The only way to resolve this issue is to introduce a non-Maxwellian electron velocity distribution. As we know, the fast solar wind is accelerated by ion cyclotron waves possibly generated by the interaction and reconnection between open flux and small-scale closed loops. Once ions are perpendicularly heated by ion cyclotron waves and execute large gyro-orbits, density gradients in the flow can excite lower hybrid waves through which electrons can then be heated in the parallel direction (Laming & Lepri 2007). A weak temperature gradient can lead to the development of non-Maxwellian suprathermal tails on electron velocity distributions, invalidating the Spitzer-Harm theory (Scudder & Olbert 1983). Therefore, solar magnetic activity might be a reason to cause the non-Maxwellian velocity distribution of electrons in the fast solar wind. But things would be different in the slow solar wind because slow solar wind plasma is believed to accumulate in closed loops for hours to days before being set free into the heliosphere. The ions execute sufficient heating in the loops and their distributions become almost isotropic. The conditions for exciting lower hybrid waves might not be satisfied. Thus the charge state in the slow solar wind would display different signatures from that in fast solar wind. The work presented in this Letter is to check the signatures of the solar magnetic activity on the charge states of heavy ions in the slow and fast solar wind.

2. DATA ANALYSIS AND RESULTS

The photospheric magnetic field is extrapolated into a global heliospheric field by using the "current sheet source surface" (CSSS) model (Zhao & Hoeksema 1995). This model uses Bogdan & Low's solution (Bogdan & Low 1986) for a magnetostatic equilibrium to calculate the effect of large-scale horizontal currents flowing in the inner corona and, by introducing the cusp surface and the source surface, uses Schatten's technique (Schatten 1971) to calculate the effects of the coronal and heliospheric current sheets and volume currents. These currents maintain the total pressure balance between regions of high and low plasma density. To model the effects of volume and sheet currents on the coronal magnetic field, the solar atmosphere is divided into three parts, separated by two spherical

[1] Solar Magnetism and Activity Group, National Astronomical Observatories, Chinese Academy of Sciences, 20A Datun Road, Chaoyang District, Beijing 100012, China; xywang@ourstar.bao.ac.cn.

[2] Max-Planck-Institut für extraterrestrische Physik, D-85740 Garching, Germany; berndt.klecker@mpe.mpg.de.

[3] Physikalisches Institut der Universität Bern, CH-3012 Bern, Switzerland; peter.wurz@space.unibe.ch.

surfaces, i.e., the cusp surface and the source surface (see Fig. 1 of Zhao & Hoeksema 1995). The inner sphere, called the cusp surface, is located approximately at the height of the cusp points of coronal streamers. Above the cusp surface the coronal magnetic field is open everywhere. The outer sphere, called the source surface, is located near the reference height identified in Parker's model above which the radially directed solar wind totally controls the magnetic field (Parker 1958). The cusp point is not easily defined and probably varies from place to place. However, the estimates of the height of cusp points from different experiments range from below 1.5 $R_\odot$ to above 3 $R_\odot$ (Zhao & Hoeksema 1995). For instance, typical coronal streamers in the K corona are approximately radial structures extending beyond 1.5–2.0 $R_\odot$. This implies a wide height range of open and closed field line interactions. Recently, Laming & Lepri (2007) pointed out that any heating mechanism for electrons between 1.5 and 3 $R_\odot$ needs to explain the discrepancy between the SUMER observations and *Ulysses* SWICS data in the fast wind. If most of the cusp points are located within 1.5–3 $R_\odot$, this implies that waves generated by the reconnection of open and closed flux will further power the solar wind beyond the point where it can be observed by SUMER; i.e., ions are heated by ion cyclotron resonant Alfvén waves and part of the energy then leaks to electrons through a collisionless process (Laming 2004). This would provide a reasonable explanation of the charge state issue in the fast solar wind (Laming & Lepri 2007).

There are two essential advantages of the CSSS model over the potential field source surface (PFSS) model: first, the field lines are open but not necessarily radial at the cusp surface, which includes the effects of streamer current sheets; second, the source surface in the CSSS model is placed near the Alfvén critical point. In situ observations of the heliospheric magnetic field should be compared with the magnetic neutral line near the Alfvén critical point. The radial component of the heliospheric magnetic field, as detected by *Ulysses*, is latitude independent (Smith & Balogh 1995) and can be taken as uniform on a spherical surface above 5 $R_\odot$ (Suess & Smith 1996). However, the magnetic field distribution on the source surface obtained using the PFSS model is not uniform, which does not agree with the *Ulysses* observations of the heliospheric magnetic field (Poduval & Zhao 2004). In addition, the CSSS model shows better prediction of solar wind and interplanetary magnetic field (IMF) polarity and intensity measured near the Earth's orbit than the PFSS model. The correlation coefficient between the observed interplanetary magnetic field and the calculated 27 day averages is 0.89 for the CSSS model, which is better than that of the PFSS model, which is 0.77 (Zhao & Hoeksema 1995). To yield uniform magnetic field on the source surface, we set the source surface at 15 $R_\odot$ (Zhao et al. 2002) and the optimum cusp surface is determined by matching trial calculations of Carrington-rotation-averaged open magnetic flux with in situ solar wind speed.

SOHO MDI daily magnetic field synoptic data is used to obtain the daily proportion of open magnetic flux on the front side of the photosphere (Fig. 1*a*) during the 23rd solar cycle [$alpha = opnf/(opnf + clsf)$, where *opnf* (*clsf*) indicates open (closed) flux on the front side of the photosphere]. The correlation of *alpha* with the sunspot number is displayed in Figure 1*b*. In this Letter we use the parameter *alpha* to describe the intensity of solar activity.

The observed solar wind is traced back to the source surface in the corona along the Archimedian spiral assuming little radial acceleration (constant speed) and pure radial flow, neglecting interaction between fast and slow solar wind streams. That is, the heliographic latitude at the source surface is the same as that of the in situ observed point. The Carrington longitude at the source

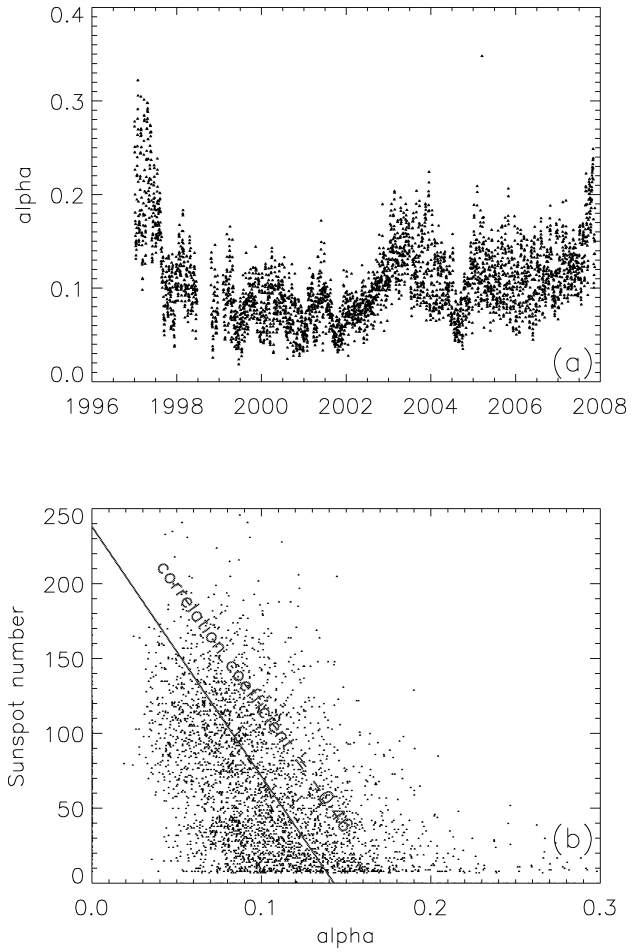

FIG. 1.—(*a*) Proportion of the open magnetic flux on the front side of photosphere: *alpha* (for the definition of *alpha* see text) as a function of time during solar cycle 23. (*b*) Correlation of the daily open flux with the daily sunspot number. [*See the electronic edition of the Journal for a color version of this figure.*]

surface is shifted to the west according to the daily values of the in situ observed solar wind speed (Neugebauer et al. 2002). Here *ACE* SWEPAM daily average solar wind data are used to infer the longitude shift. Once the shifted longitude is obtained, we get the time of day that the solar wind comes out of the source surface, and we further get the daily fraction of open magnetic flux on the front side of photosphere on that day. By this mapping technique, in situ observed solar wind is associated with low, middle, and high solar magnetic activity, i.e., $alpha > 0.14$, $0.075 < alpha < 0.14$, and $alpha < 0.075$, respectively. We do not use the inverse relation between flux tube expansion factor and solar wind speed, because the solar wind will be tracked back to a region bounded within a narrow range of longitude that sensitively depends on the mapping speed used, but rather emphasize the influence of the background magnetic field on the properties of solar winds, i.e., the fraction of the open flux on the front side of the photosphere.

Note that the solar wind speed profile obtained at 1 AU is the result of the interaction between solar winds of different speeds as they propagate outward and the stream-stream interactions are inevitable. Our constant-speed assumption would inevitably introduce longitude shift errors and cause a possible wrong mapping of solar wind with solar activity. However, we use the daily synoptic MDI data for the mapping, which weakens the influence of the longitude shift error to some degree. For instance, an error of less than 13° would not change the mapping result.

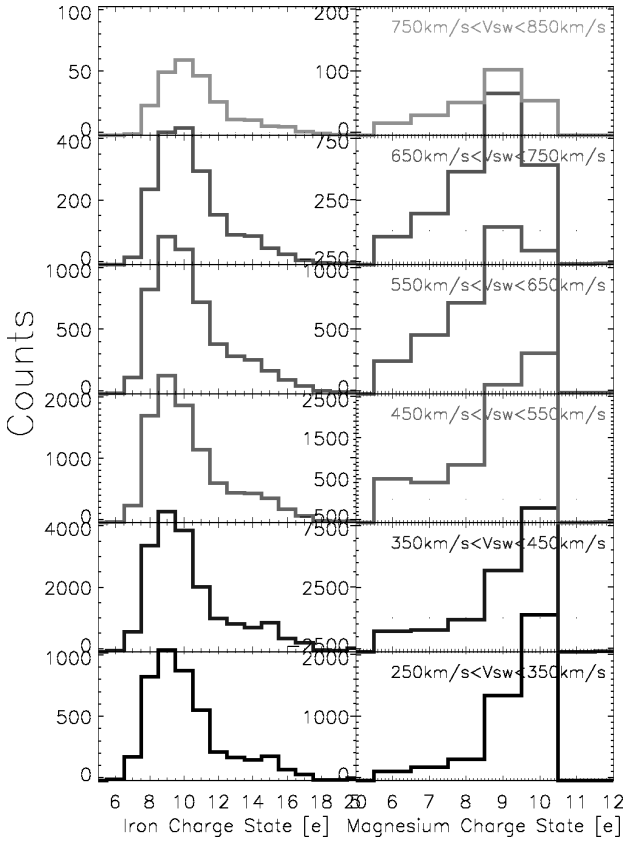

FIG. 2.—Charge state distributions of Fe and Mg of the solar wind (without ICMEs) for six speed bins from 250 to 850 km s^{-1} during solar cycle 23. [*See the electronic edition of the Journal for a color version of this figure.*]

We analyzed *ACE* SWICS charge state distributions of heavy ions, Fe, Si, Mg, Ne, O, and C, from the years 1998 to 2007. The criterium $O^{+7}/O^{+6} < 0.8$ is used to separate interplanetary coronal mass ejections (ICMEs) from the quasi-stationary solar wind based on the results by Richardson & Cane (2004). The corresponding charge state distributions of Fe and Mg of the solar wind for six different speed ranges are compiled in Figure 2. The wide range of charge states of the measured distribution is due to a mix of sources in the solar wind. As the solar wind speed increases, two opposite trends are identified: for iron, a charge state peak shifts from $Q = 9$ to $Q = 10$ with a tail extending to $Q = 20$; for magnesium, the charge state peak shifts from $Q = 10$ to $Q = 9$ with a tail extending to $Q = 5$. The opposite trend for Fe and Mg may be due to the effects of resonant acceleration at high altitude in the corona, where the magnetic effects dominate and preferentially select species with lower charge state (that is, with higher m/q) in the slow solar wind. The slow solar wind plasma is believed to accumulate in closed loops for hours to days before being released into the heliosphere by the interchange reconnection with open flux. The heating will occur in the loops of the corona by the interaction of ions with MHD turbulence. If ions are heated by magnetic fluctuations with a power-law spectrum $P(\omega) \propto \omega^{-\lambda}$, the ions with higher m/q will be heated more strongly. Therefore, we see lower charge states of Fe ions in the slow solar wind. However, the m/q for Mg is nearly half of that for Fe, which implies less power at the Mg resonances. As a result, the resonant heating at high altitudes of the corona is much less efficient for Mg than for Fe. So the charge distribution of Mg, dominated by Mg^{10+} over a wide range of T_e, still keeps the information of the source temperature of the inner corona, with a different trend for Fe.

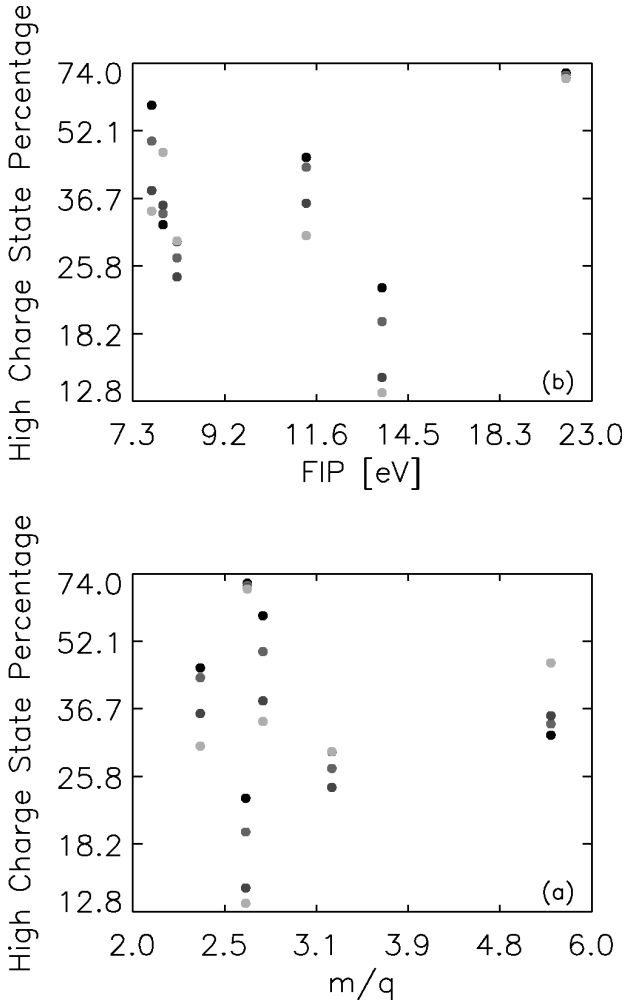

FIG. 3.—(*a*) Mean charge states for four speed bins as a function of m/q (*black*, 250–350 km s^{-1}; *green*, 350–450 km s^{-1}; *red*, 450–550 km s^{-1}; *yellow*, 650–750 km s^{-1}). (*b*) Mean charge state for four speed bins as a function of FIP. [*See the electronic edition of the Journal for a color version of this figure.*]

To explore the magnetic effects on the m/q distribution, we calculated the mean charge states within different speed bins as a function of m/q, which are displayed in Figure 3*a*. For comparison, the dependence on the first ionization potential (FIP) is given in Figure 3*b*. We find that the fractions of the high charge states ($Q_{Fe} > +10$, $Q_{Mg} > +7$, $Q_{Si} > +7$, $Q_{Ne} > +7$, $Q_O > +6$, $Q_C > +5$)increase with the solar wind speed when the m/q is above 3; below this value, the fractions decrease with solar wind speed. No significant variation is found for Ne ($m/q = 2.63$). The resonant heating of ions by magnetic fluctuations with a power-law spectrum will preferentially select species with lower charge state (higher m/q) in the slow solar wind, which leads to the higher fractions of lower charge states in slow solar wind. On the other hand, ions are perpendicularly heated by ion cyclotron resonant Alfvén waves in the fast solar wind; electrons would be heated as well through the lower hybrid waves excited by the density gradients in the flow (Laming & Lepri 2007). The increased electron temperature then further ionizes the plasma and leads to higher ionization charge states in the fast streams. Once heated by lower hybrid waves, the electron distributions would depart from a Maxwellian velocity distribution (Laming & Lepri 2007). This is consistent with the theoretical assumption of non-Maxwellian velocity distribution for electrons to solve the charge state issue in fast streams (Aellig et al. 1999; Esser & Edgar 2000). In comparing the ionic charge states for different types of solar

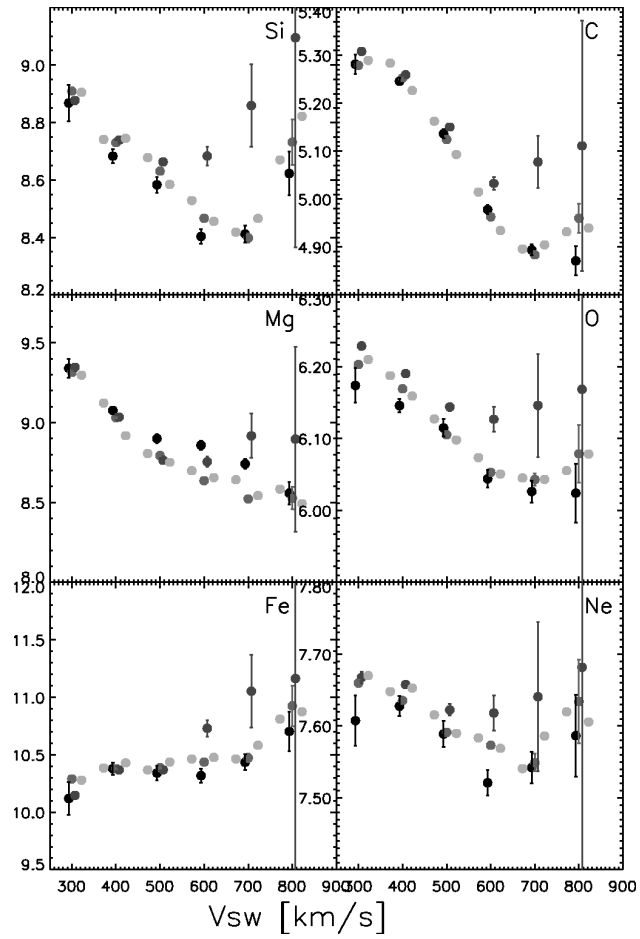

FIG. 4.—Mean charge states for Fe, Si, Mg, Ne, O, and C underlying different levels of solar magnetic activity (*black*, low activity; *green*, middle activity; *red*, high activity). Yellow points indicate the mean charge states of all solar wind bins without ICMEs. [*See the electronic edition of the Journal for a color version of this figure.*]

wind, Ko et al. (1999) found that the charge states of C and O for low-latitude fast wind ($v > 500$ km s^{-1}) are higher than those for south polar fast wind with the speed ($v > 700$ km s^{-1}), but the charge states of Si and Fe for low-latitude fast wind are lower than those for south polar wind (see Fig. 5 of their paper). This result does not violate the m/q-dependent response of the charge states to the magnetic effects in the fast solar wind, although the authors attributed the difference to either lower ion velocity or higher electron density toward lower latitude, rather than the electron temperature. They also compared the charge states for low-latitude slow solar wind to those of south polar wind. But they did not show lower charge states for Fe in the slow solar wind (see Fig. 6 of their paper), as do our observations. The discrepancy is likely due to either the latitude dependence of the charge states in the fast wind or the possibility that the solar activity dependence of the charge states is more significant in low latitude than in high latitude. Further investigation of this issue needs a combined data set observed from low latitude to high latitude.

Mean charge states for all six heavy ions underlying different levels of solar magnetic activity are compiled in Figure 4, in which the black, green, and red points in the electronic edition of the *Journal* correspond to low, middle, and high levels of solar activity, respectively, as defined above. The speed intervals correspond to the ones indicated in Figure 2. The error is the 1 σ error of the mean charge state. When the solar activity is high, the error bars are large in the fast solar wind. However, for solar wind speeds below 700 km s^{-1}, the mean charge states still reveal a significant overall variation of the charge states with solar activity. The yellow points in Figure 4 (in the electronic edition of the *Journal*) correspond to the mean charge states, averaged over all three solar activity cases with a half speed interval of Figure 2. The mean charge states are significantly solar activity dependent when the solar wind speed is above 550 km s^{-1}. At lower speeds, no significant solar activity dependence is found. Also, when plotted as a function of solar wind speed, the mean charge states for iron display a trend of increasing with solar wind speed, and on the contrary, for magnesium display a trend of decreasing with speed. For the other four ions (Si, Ne, O, C) this trend changes from negative speed dependence to positive speed dependence at the point near 675 km s^{-1}.

3. CONCLUSIONS

We presented several interesting findings in this Letter: first, we observe a dependence of the charge state distribution of heavy ions with the solar activity. This dependence is more significant in fast solar wind than that in slow solar wind; second, iron is different from other species in that it displays lower charge states in slow wind than in fast wind; third, the fractions of the high charge states for Fe and Si ($Q_{\rm Fe} > +10$, $Q_{\rm Si} > +7$) increase with the solar wind speed, while for the species with lower m/q, the fractions of the high charge states ($Q_{\rm Mg} > +7$, $Q_{\rm O} > +6$, $Q_{\rm C} > +5$) decrease with the solar wind speed.

We thank the anonymous referee for valuable suggestions and comments that helped improve the manuscript. We thank the *ACE* SWICS-SWIMS instrument team and the *ACE* Science Center for providing the *ACE* data. X. W. thanks Xuepu Zhao at Stanford University for providing the CSSS model and Yuzong Zhang at NAOC for help in understanding the model. This work is supported by the National Basic Research Program of China (2006CB806303).

REFERENCES

Aellig, M. R., et al. 1999, Phys. Chem. Earth C, 24, 407
Arnaud, M., & Raymond, J. 1992, ApJ, 398, 394
Bogdan, Y. J., & Low, B. C. 1986, ApJ, 306, 271
Bryans, P., et al. 2006, ApJS, 167, 343
Chen, Y., Esser, R., & Hu, Y. 2003, ApJ, 582, 467
Esser, R., & Edgar, R. J. 2000, ApJ, 532, L71
———. 2001, ApJ, 563, 1055
Fisk, L. A. 2003, J. Geophys. Res., 108, 1157
Fisk, L. A., & Zurbuchen, T. H. 2006, J. Geophys. Res., 111, A09115
Fisk, L. A., et al. 1999, J. Geophys. Res., 104, 19765
Ko, Y.-K., et al. 1997, Sol. Phys., 171, 345
———. 1999, J. Geophys. Res., 104, 17005
Laming, J. M. 2004, ApJ, 604, 874
Laming, J. M., & Lepri, S. T. 2007, ApJ, 660, 1642
Neugebauer, M., et al. 2002, J. Geophys. Res., 107, 1488
Owens, M. J., et al. 2007, Geophys. Res. Lett., 34, L06104
Parker, E. N. 1958, ApJ, 128, 664
Poduval, B., & Zhao, X.-P. 2004, J. Geophys. Res., 109, A08102
Reames, D. V. 1999, Space Sci. Rev., 90, 413
Richardson, I. G., & Cane, H. V. 2004, J. Geophys. Res., 109, A09104
Schatten, K. H. 1971, Cosm. Electrodyn., 2, 232
Scudder, J. D., & Olbert, S. 1983, in Solar Wind Five, ed. M. Neugebauer (NASA CP-2280; Washington: GPO), 163
Smith, E. J., & Balogh, A. 1995, Geophys. Res. Lett., 22, 3317
Suess, S. T., & Smith, E. J. 1996, Geophys. Res. Lett., 23, 3267
Zhao, X.-P., & Hoeksema, J. T. 1995, J. Geophys. Res., 100, 19
Zhao, X.-P., Hoeksema, J. T., & Rich, N. B. 2002, Adv. Space Res., 29, 411